Langmuir

Article

Tailoring the Protein Adsorption Properties of Whispering Gallery Mode Optical Biosensors

Carol Elaine Soteropulos, Kevin M. Zurick, Matthew T. Bernards, and Heather Hunt

Langmuir, **Just Accepted Manuscript** • Publication Date (Web): 12 Oct 2012

Tailoring the Protein Adsorption Properties of Whispering Gallery Mode Optical Biosensors

Carol E. Soteropulos,[†] Kevin M. Zurick[‡], Matthew T. Bernards,[†‡] Heather K. Hunt[†]*

†Department of Biological Engineering, University of Missouri, 1201 Rollins Street, 240G, Columbia, MO 65211, United States

‡Department of Chemical Engineering, University of Missouri, W2011 Lafferre Hall, Columbia MO, 65211, United States

Email: hunthk@missouri.edu

RECEIVED DATE

Label-free biosensor technologies have the potential to revolutionize environmental monitoring, medical diagnostics, and food safety evaluation processes due to their unique combinations of high sensitivity signal transducers and high specificity recognition elements. This enables their ability to perform real-time detection of deleterious compounds at extremely low concentrations. However, to further improve the biosensors' performance in complex environments, such as wastewater, blood, and urine, it is necessary to minimize non-specific binding, which in turn will increase their specificity, and decrease the rate of false positives. In the present work, we illustrate the potential of combining emerging high sensitivity optical signal transducers, such as Whispering Gallery Mode (WGM) microcavities, with covalently-bound poly(ethylene-glycol) (PEG) coatings of varying thickness, as an effective treatment for the prevention of non-specific protein adsorption onto the biosensor surface. We monitor the sensitivity of the coated biosensor, and investigate the effect of PEG chain length on minimizing non-

specific adsorption via protein adsorption studies. Experimental results confirm not only that PEG-functionalization reduces non-specific protein adsorption to the surface of the sensor by as much as a factor of four compared to an initialized control surface, but also that chain length significantly impacts the non-fouling character of the microcavity surface. Surprisingly, it is the short chain PEG surfaces that experience the best improvement in specificity, unlike many other systems where longer PEG chains are preferred. The combination of WGM microcavities with PEG coatings tuned specifically to the device will significantly improve the overall performance of biosensor platforms, and enable their wider application in complex, real-world monitoring scenarios.

KEYWORDS Optical Microcavity, Microsphere, Whispering Gallery Mode, Biosensor, Poly(ethylene-glycol), Nonspecific Adsorption, Nonfouling Surface

Introduction

Poly(ethylene-glycol) (PEG) is a widely-studied and versatile biocompatible polymer, which has applications in a wide range of scientific arenas, such as PEG-protein conjugates for pharmaceutical applications, PEG hydrogels utilized for drug delivery and wound healing, and PEG tethering for cell signaling and targeting.[1] The most widespread application for PEG, however, makes use of its ability to create protein-resistant, or nonfouling, surfaces from otherwise protein-attractive materials via its strong hydration layer and steric stabilization effect.[1-5] This has resulted in intense interest from the biomedical community for creating medical devices, implants, and biomaterials, which would all greatly benefit from the minimization of protein adsorption and cell adhesion on their surfaces to avoid promotion of an immune response.[1, 6-7] However, the functionality of these properties is not limited to implantable devices, but extends to any surface platform that interacts with biological species, and could suffer from surface fouling due to non-specific adsorption.

For instance, PEG has been widely used to improve the specificity of optical biosensing platforms, such as commercial surface plasmon resonance (SPR) sensors, and silica nanoparticles.[8-13] PEG has also been shown to have nonfouling properties that are on par with other nonfouling functional groups, even

in the presence of complex media.[14] To create a successful, commercial optical biosensing platform, a high sensitivity signal transducer (or sensor) must be coupled with a high specificity recognition element (such as an antibody), to enable the detection of a specific pathogen in a very complex environment, such as blood, urine, wastewater, etc.[15] Although these biosensing platforms are typically tailored to a specific target, random non-targeted bioactive molecules can still adsorb onto the surface of the biosensing platform via non-specific physical, chemical, or electrostatic adsorption.[2, 16] This can result in high rates of false positives, a decrease in the signal to noise ratio, and a reduction in the function of the device in a non-laboratory environment.[17] Creating nonfouling backgrounds, by coating them with PEG during the attachment of the recognition element, can greatly enhance the performance of the platform by regaining the theoretical specificity that the recognition element alone should lend to the platform.[3-4, 9, 12, 18] This enables the transition of many such optical biosensing platforms from the laboratory to real-world application.

Recently, an emerging class of high sensitivity optical signal transducers, known as Whispering Gallery Mode (WGM) microcavities, has demonstrated intriguing capabilities as the foundation of label-free optical biosensing platforms.[15, 19-24] These devices, which can be fabricated in many micro-scale geometries (microrings, microdisks, microtoroids, microspheres, etc.), efficiently confine a circulating optical field at specific resonant frequencies within the device periphery.[25] As the optical field circulates, it extends into the surrounding environment through evanescence, and can interact with biomolecules as they adsorb on or bind to the surface. Binding or adsorption events result in the modification of the effective refractive index of the circulating optical field, causing a detectable shift in the resonant frequency of the device.[26-29] This enables the sensing capabilities of the devices. Their ultra-high sensitivities derive from their very low optical loss, and therefore long photon lifetimes in the microcavity, which increase the interaction between the circulating photons and biomolecules in the surrounding environment.[28, 30] This results in higher sensitivity than conventional label-free optical biosensing platforms, such as SPR.[19] Previous research using such optical cavities has demonstrated

their application as a platform for molecular detection of an array of biologically-relevant species, with the ability to detect at ultra-low concentrations.[15, 31]

Despite their enormous potential for creating next-generation, label-free optical biosensing platforms, WGM microcavities lag behind their more mature counterparts, such as SPR platforms, due to their relatively recent emergence in the field.[31] PEG technology has recently begun to be applied to these devices, primarily to increase cell viability on the surface of such devices, but has yet to be applied to determine how best to tailor the surface to minimize protein adsorption.[32] Although PEG coatings have been proven to minimize nonspecific adsorption on various classes of biosensors, the impact of their chain length and attachment has yet to be investigated for this new class of high-sensitivity WGM microcavities, thus limiting the use of such high potential devices in complex environments. In particular, given the complex, three-dimensional nature of the WGM microcavities in comparison to planar optical biosensors, such as SPR platforms, translating typical surface chemistries from homogeneous solution chemistries to three-dimensional heterogeneous chemistries, such as PEG coatings to minimize non-specific adsorption, is often challenging, as simple things like the shear force generated by slow stirring can damage three-dimensional surfaces. Therefore, the optimal conditions for planar and three-dimensional platforms are often different. Moreover, due to the high sensitivity of these signal transducers, it is necessary to demonstrate that such coatings will not negatively impact the overall sensitivity of the platform in an effort to improve the specificity. In the present work, we look to further the utility and sensitivity of these WGM microcavity-based optical biosensors through the creation of nonfouling surfaces using silane-PEG molecules. We successfully demonstrate the ability of the PEG-functionalized devices to prevent non-specific protein adsorption, and subsequently probe the influence of PEG chain length on adsorption and device performance.

Materials and Methods

Device fabrication and functionalization

The silica microspheres used in this work were fabricated by gravimetric melting of the tip of an single-mode optical fiber (Newport, F-SC-C-1FC) with a 25 W CO_2 laser operating at 6 – 8% output power.[30,33] The microspheres were functionalized with poly(ethylene-glycol) (PEG) molecules of different molecular weights, and therefore, different film thicknesses, using a two-step covalent attachment process shown in Figure 1a (see Supplemental Information for more detail).[34-35]

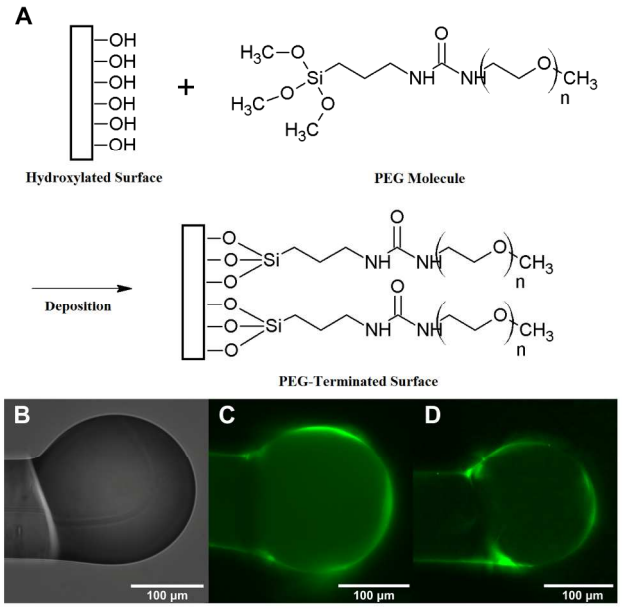

Figure 1. a) Functionalization process used to coat the surface of the microsphere with MPEOPS and PEG-5000, b) brightfield image of a functionalized microsphere indicating minimal surface imperfections, c) fluorescent image of a microsphere coated with silane-PEG-FITC (M_w = 400) shows uniform and robust coverage of PEG, and d) fluorescent images of a microsphere coated with silane-PEG-FITC (M_w = 5000) confirming the success of PEG attachment protocols at both low and high molecular weight.

The microsphere surface was then PEG-terminated using silane-PEG molecules of both low and high molecular weight. In the present work, we used 2-[Methoxypoly(ethyleneoxy)propyl] trimethoxysilane (MPEOPS, M_w = 460-590, purity > 90%, Gelest), and Methoxyl silane poly(ethylene-glycol) (PEG-5000, M_w = 5000, Nanocs) as the silane-PEG chains under investigation. To determine the best deposition technique for our three-dimensional, WGM biosensor platform, we evaluated various solvent

and vapor deposition conditions reported in literature for planar surfaces (Table 1, see Supplemental Information for more detail).

Trial	Deposition	PEG Molecule	Concentration	Temperature (°C)	Time (hr)
1	Vapor	MPEOPS	100%	25	3
2	Vapor	MPEOPS	100%	25	7
3	Solvent	MPEOPS	10%	25	3.5
4	Solvent	MPEOPS	10%	95	3.5
5	Solvent	PEG-5000	5 mg/mL	25	3.5
6	Solvent	PEG-5000	5 mg/mL	95	3.5

Table 1. Reaction Conditions Examined for PEG Attachment

Characterization of PEG Attachment

To characterize the success of the PEG-functionalization process, both fluorescence microscopy and ellipsometry, in conjunction with protein adsorption, were used. Additionally, atomic force microscopy was used to evaluate the quality of the functionalized surfaces (see Supplementary Information). To confirm uniform PEG coatings on the surface of the microspheres, we attached silane-PEG molecules of molecular weight similar to those used in the present work (M_w = 400, 5000), conjugated to fluorescein isothiocyanate (FITC) (Nanocs), through the previously described methods. The protocols were slightly modified due to the nature of the low molecular weight silane-PEG-FITC, which arrived in chloroform from the manufacturer and was further diluted to the appropriate concentration using chloroform (Sigma Aldrich) instead of toluene. Imaging was performed using an inverted fluorescent microscope (Olympus IX70), along with MetaMorph image acquisition and analysis software. A filter set (Chroma Technology Corp.) corresponding to the excitation/emission profile of FITC was also used (41001 FITC/EGFP/Bodipy Fl/Fluo3/DiO). The fluorescently labeled microsphere was mounted above a glass coverslip, through which the fluorescent images were taken. Thickness measurements were completed using a Variable Angle Spectroscopic Ellipsometer (J.A. Woollam Co. VB400/HS-190), with data taken at angles of 60°, 65° and 70°. Ellipsometry data was fit and analyzed using a Cauchy model.

The initial protein adsorption study was done utilizing silica-on-silicon (100) wafers (University Wafer), with a 2 um silica (thermal oxide) grown on the surface, as control surfaces that model the silica microsphere optical resonator surface. This perfectly smooth and reflective surface allowed us to determine surface coating thicknesses and changes after protein adsorption using ellipsometry. As previously discussed, the different attachment protocols were examined using this model surface in order to find the protocol best suited for translation from the flat, robust wafer surface to the 3-dimensional, contamination-prone surface of the microsphere (Table 1). The initial PEG film thickness was determined through ellipsometry using the polished side of the silica-on-silicon (100) wafers that had been hydroxylated (initialized) through the piranha etch, and subsequently functionalized with either MPEOPS or PEG-5000 through each of the protocols described in Table 1. Both PEG-functionalized and hydroxylated control wafers were then immersed in 1 mg/mL solutions of lysozyme (chicken egg white, Sigma Aldrich) and fibrinogen (bovine plasma, EMD Chemicals) in phosphate buffered saline (PBS, EMD Chemicals) for one hour, after which they were rinsed copiously with PBS and blown dry with N_2. Following protein adsorption, a final thickness measurement was taken. Protein adsorption was calculated by subtracting the initial thickness from the final thickness.[2]

Device Characterization

To confirm the optical performance of the as-fabricated and functionalized microspheres, the quality factor (Q) was measured before and after PEG deposition. The Q factor quantitatively describes the photon lifetime within the microcavity, and is the figure of merit by which device sensitivity is reported. In order to calculate the Q factor, the whispering gallery modes of the silica microspheres were excited by the coupling of optical power from a narrow linewidth, tunable, diode laser centered at 980 nm (New Focus), via a single-mode, tapered optical fiber (Newport, F-SC-C-1FC).[30, 36-37] The tapered fiber was fabricated through simultaneous stretching and heating of the fiber using a hydrogen torch (Premier Industries) while stretching the fiber with a two-axis stage controller (Sigma Koki) until an average waist diameter of ~800 nm is reached.[36] This method of evanescent coupling minimizes extrinsic microcavity losses (losses due to improper coupling, rather than the microcavity itself), which could

negatively impact the Q factor.[36] The coupling distance between the tapered optical fiber and the silica microsphere was maintained by placing the microsphere on a 3-axis nanopositioning stage (Optosigma), while monitoring the system with both side- and top-view cameras simultaneously. The transmission data was visualized using an oscilloscope integrated into the computer system (NI, PCI-5114), and the resonant wavelength was recorded in the under-coupled regime, where extrinsic coupling loss was minimized and less than the intrinsic loss of the microcavity, under optimal laser scan speed and scan direction, which ensured that neither distorted the resonance lineshape (Figure 2).[37-39] A Lorentzian fit of the resonant peak data is used to calculate the linewidth (full width at half-maximum). The Q factor was then calculated from the resonance peak using the following equation:

$$Q = \frac{\lambda}{\Delta\lambda} \qquad \text{Equation 1}$$

where $\Delta\lambda$ is the linewidth (full width at half-maximum) value obtained from the Lorentzian fit of the resonant peak data, and λ is the resonant wavelength.

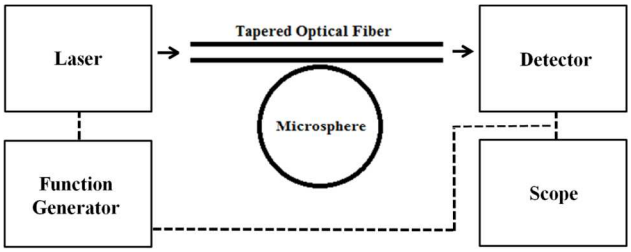

Figure 2. Schematic detailing experimental setup for monitoring of optical performance of microsphere optical microcavities.

Sensing and prevention of non-specific binding

Protein sensing experiments were performed through the creation of a buffer-filled microaquarium described in detail in previous literature and shown in Figure 3.[40-41] The microsphere-taper system was immersed in PBS through attachment of a coverslip on top of the system. A syringe pump was used to inject varying concentrations of protein solutions from directly below the microsphere-taper system, using previously determined experimental flow conditions.[41] Solutions of lysozyme or fibrinogen were created at concentrations of 10, 100, 500 and 1000 μg/mL in PBS. During these experiments, a resonant

peak was found and focused upon through alignment with the tapered optical fiber, while a custom LabVIEW program recorded the lowest point on the oscilloscope graph of transmission voltage versus time throughout the experiment. The data recorded from this program allowed for visualization of the resonant shift as a function of time prior to injection, during protein injection, and after completion of injection. Therefore, we were able to track the shift in the resonant frequency throughout the entire sensing experiment. Additional control experiments were conducted where a PBS buffer rinse was injected into the sensor following the protein injection step. All other procedures were identical.

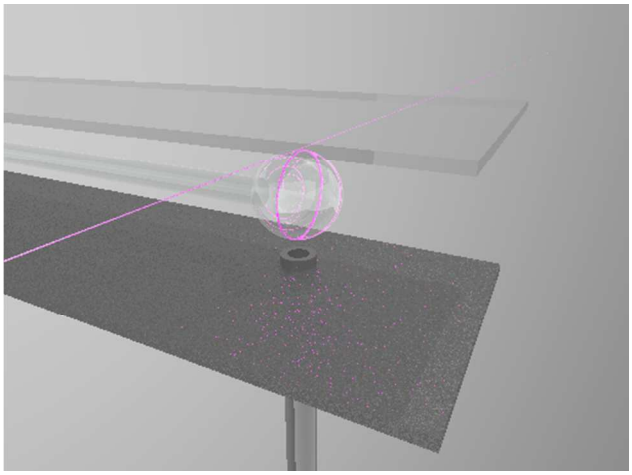

Figure 3. Schematic of the microaquarium housing for the microsphere-taper system, used during protein adsorption sensing experiments.

Results and Discussion

Covalent attachment of PEG

To verify the thickness of the PEG coatings resulting from various deposition techniques, the functionalization procedures were applied to flat (control) silica-on-silicon wafers, as previously described. A protein adsorption study was performed in conjunction with ellipsometry to confirm that the PEG-functionalized surfaces were indeed resistant to protein adsorption using lysozyme and fibrinogen as the model proteins of interest. Thickness measurements were recorded before and after PEG-functionalized silica wafers were exposed to 1 mg/mL solutions of lysozyme and fibrinogen, and subsequently rinsed with PBS. These measurements allowed calculation of the thickness of the adsorbed protein layer through subtraction of initial from final thickness. Figure 4 shows that in

comparison with the hydroxylated control, the surfaces functionalized through solvent deposition of both MPEOPS and PEG-5000 greatly reduced protein adsorption at each concentration and temperature examined. In addition, Figure 4 shows that vapor deposition of MPEOPS was not successful in comparison to the other techniques at minimizing adsorption; a significant amount of protein adsorbed to the surface, which could indicate that the short chain PEG was indeed too heavy to be vaporized with minimal effort, resulting in poor surface uniformity or coverage. Therefore, vapor deposition of PEG-5000 was not tested. Based on these results, we selected the solvent deposition attachment techniques for both MPEOPS and PEG-5000, performed at room temperature, to maximize ease and efficiency of PEG attachment and minimize protein adsorption. The detailed experimental conditions of the chosen protocols for MPEOPS and PEG-5000 attachment are shown in Trials 3 and 5 of Table 1, respectively. The average thicknesses of the MPEOPS and PEG-5000 coatings resulting from these trials were measured with ellipsometry to be 11.03 nm (+/- 2.17) and 3.33 nm (+/- 0.395) respectively, which is in good agreement with existing literature.[34-35] The protein adsorption study in conjunction with ellipsometry further confirmed uniform and dense PEG coverage, as well as the ability of both PEG-functionalized surfaces to resist non-specific binding of both lysozyme and fibrinogen at high concentrations.

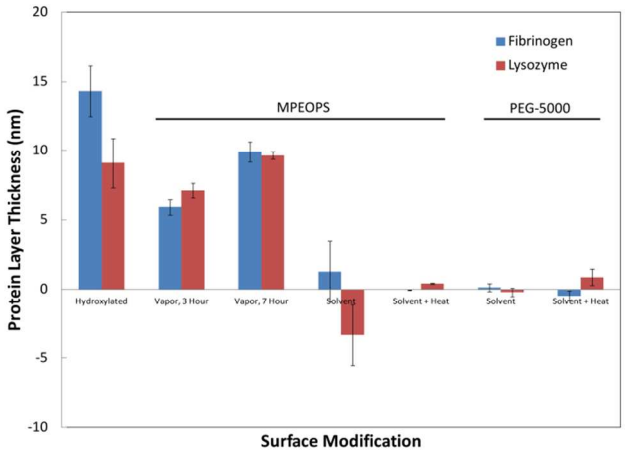

Figure 4. Mean thickness of the adsorbed protein layer (± standard deviation) adsorbed onto silica surfaces that were functionalized through various protocols as measured via ellipsometry (n=3). It is

evident that solvent deposition of PEG (M_w = 450 and M_w = 5000) at both room temperature and with heat (95°C) effectively reduces protein adsorption as compared to the hydroxylated control.

After careful examination of all potential PEG functionalization protocols using silica-on-silicon wafers, the selected protocols (Trials 3 and 5) were applied to the silica microspheres. To verify the impact of the coating on the surface, optical microscopy was used to determine the final quality of the sphere surface, post-functionalization, as surface defects and debris are known to negatively impact the sensitivity of the device via quality factor reduction.[30] As shown in Figure 1b these protocols resulted in functionalized microsphere surfaces that were clean and free of imperfections. In order to confirm robust and uniform surface coverage of the PEG coating, fluorescence microscopy was used to image the microspheres after functionalization with PEG molecules labeled with fluorescein isothiocyanate (FITC) of similar molecular weight to those used in this study. As seen in Figure 1c and Figure 1d, silane-PEG-FITC coverage was indeed robust and uniform across the microsphere surface, thus confirming the success of the PEG functionalization method used for both molecular weights (M_w = 550 and M_w = 5000).

Maintenance of device sensitivity

In order to verify that the functionalized devices remained sensitive enough to perform detection studies, the Q factor was measured for six different microspheres after MPEOPS or PEG-5000 attachment. A typical transmission spectrum, obtained from raw oscilloscope data of an on-resonance microsphere, is shown in black on Figure 5 (inset), with the Lorentzian fit shown in red. Previous literature has shown that a Q factor of 10^6 or higher ensures that the functionalized devices are capable of detection of single viruses and nanoparticles; this level of sensitivity allows for detection of biomolecules at biologically relevant conditions.[31] Figure 5 shows that quality factor remains above 10^6 for a set of 10 microspheres functionalized with either MPEOPS or PEG-5000, confirming the sensitivity to be high enough for use in protein adsorption studies.

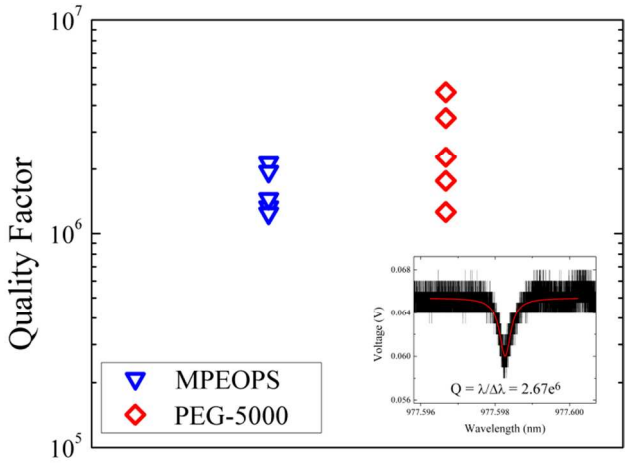

Figure 5. Optical performance of a series of microspheres after functionalization with either MPEOPS or PEG-5000 measured through the Q factor of the device. All microspheres present a Q factor of above 10^6, confirming sufficient sensitivity for use in subsequent protein adsorption experiments. (Inset) Representative graph showing raw oscilloscope data (black) of a resonant peak, and Lorentzian fit (red) of the resonant peak data. The sensitivity (Q factor) is calculated utilizing the full width at half maximum value ($\Delta\lambda$) taken from the Lorentzian fit of the data, and the resonant wavelength (λ).

Sensing and prevention of non-specific binding

The custom LabVIEW program used during sensing records the lowest point on the oscilloscope graph of voltage versus time for a microsphere on resonance, from which we are able to construct a curve showing the association of protein with the surface of the microcavity. The resonant shift observed during protein injection is related to the amount of adsorbed protein and bulk refractive index changes from the protein solution.[42-43] Sensing experiments using solutions of lysozyme or fibrinogen in PBS were initially performed at the protein concentrations stated in the Experimental Section. The concentrations that produced results most compatible with our experimental setup in terms of our ability to fully track the resonant peak shift were 500 μg/mL lysozyme in PBS, and 10 μg/mL fibrinogen in PBS. The experimental setup used more easily tracks smaller resonant shifts associated with lower concentrations of proteins, while higher concentrations will result in too large of a resonant shift to be tracked to completion (Fig. 6a). To confirm that the resonance shift seen upon protein injection was not due in part to fluid flow (the injection process itself, rather than protein adsorption, desorption, or

conformational changes), we performed additional experiments, which showed no significant shift during an injection of pure buffer, confirming that the shift seen upon injection is a direct result of protein adsorption and is in no part due to fluid flow (data not shown).

Representative curves created from the sensing data obtained from this program are shown in Figure 6; each curve consists of 3 key time points: A) protein injection begins, B) protein injection ends, and C) post-injection settling, where the resonant frequency has ceased to shift after the injection has ended. Based on the extent of the resonant shift, we can compare the PEG coatings to each other and to control surfaces (hydroxylated microspheres), and determine the success of the coating at minimizing surface fouling. We express the amount of protein adsorbed based on the resonant wavelength shift between the beginning and end of the protein injection phase (points A and B). Although other common sensing platforms (such as surface plasmon resonance sensors) calculate a resonant shift only after a buffer rinse step has been completed after point C, in the present work we found that a buffer rinse step did not generate any significant backshift with our sensing platform; rather, the resonant frequency at the settling point (C) did not change at all during or after the buffer rinse step post-settling (data not shown).

There are three potential explanations for the behavior of the shift between points (B) and (C). First, slight changes in coupling efficiency of the sensor platform, which can occur both before and after protein injection due to slight variations in the distance between the WGM microcavity and taper during the experiment (i.e. equipment drift rather than protein interaction behavior) can lead to resonant wavelength shifts. This is because a slight change in the circulating optical field of the device will result in a shift in the resonant wavelength of the platform. Second, protein desorption could cause a shift back towards the baseline resonant frequency. However, this is not expected to play a role in this system, because protein is still present in the bulk solution after injection, thus reducing the driving force for desorption to occur. This is a result of our microaquarium, which acts like a batch setup, rather than a continuous flow setup, and therefore, we do not expect this to be the major cause the shifts obtained. Third, protein conformational changes could cause such shifts. We hypothesize that because the buffer rinse did not generate a backshift, the majority of the settling backshift in this experiment is

due to a combination of changes in protein conformation, as discussed in great detail elsewhere in the literature.[11, 32, 44-45] The shift towards the original baseline resonant wavelength of the platform is likely due to some combination of these three possibilities, however, protein conformational changes are likely to play the dominant role.

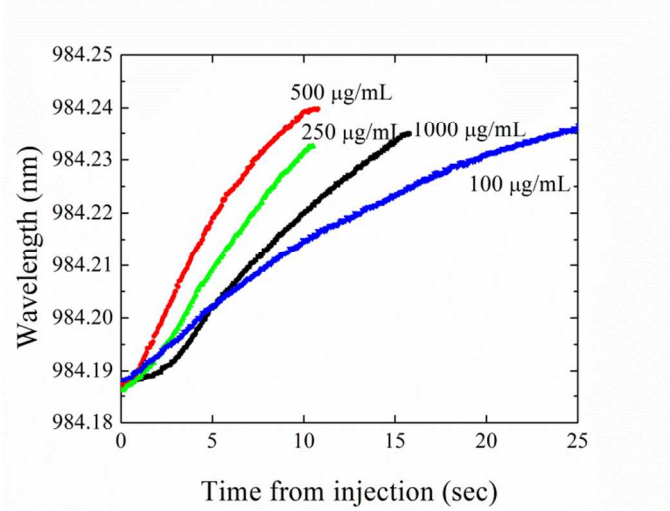

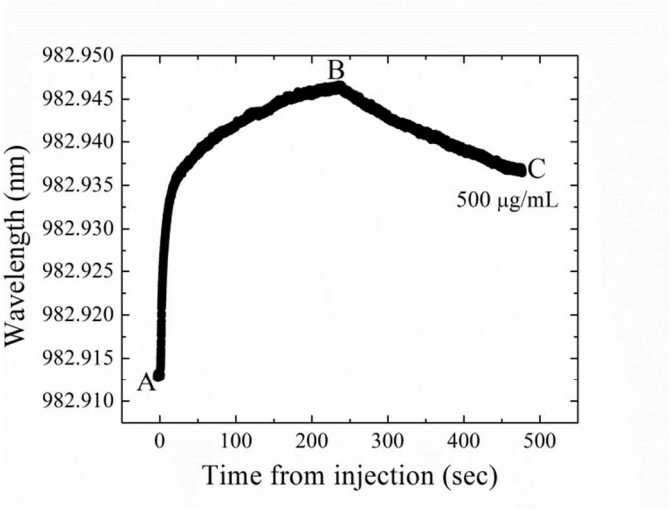

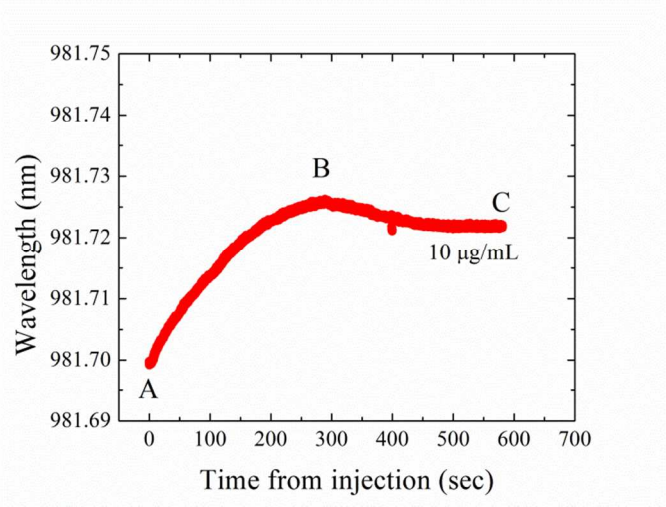

Figure 6. Representative resonant shift curves taken during protein adsorption experiments, where points (A, B, C) represent injection start time, injection end time, and settling end time, respectively. (a) Injection of fibrinogen across control (hydroxylated) microspheres, showing that high protein concentrations cause too large of a shift in the microsphere's resonant wavelength to track during the injection. (b) Injection of lysozyme across PEG-5000-functionalized microspheres. (c) Injection of fibrinogen across PEG-5000-functionalized microspheres.

The resonant wavelength shift data for experiments performed using both lysozyme and fibrinogen solutions in Figure 7 shows that the microspheres functionalized with both MPEOPS and PEG-5000 effectively reduce protein adsorption as compared to the hydroxylated control surfaces. Published literature reports that less than 1% of a monolayer of lysozyme and 35-50% of a monolayer of fibrinogen will adsorb onto a hydroxylated surface.[4] Based on these reference points, the MPEOPS coated surface had 0.5% and 11.7-16.7% of a monolayer of adsorbed lysozyme and fibrinogen, respectively. While lower levels of protein nonspecific protein adsorption have been seen with PEG functional groups and others, these previous studies have been focused on planar geometries (ellipsomentry, SPR, etc.) which are easier to passivate than the complex three-dimensional geometry associated with the WGM biosensor platform.

The resonant shift data further show that the short chain PEG coating (MPEOPS) is more effective at reducing both lysozyme and fibrinogen adsorption on the surface of the microsphere in comparison to

the long chain PEG coating (PEG-5000). It is interesting to note that this result is somewhat atypical for PEG functionalized surfaces.

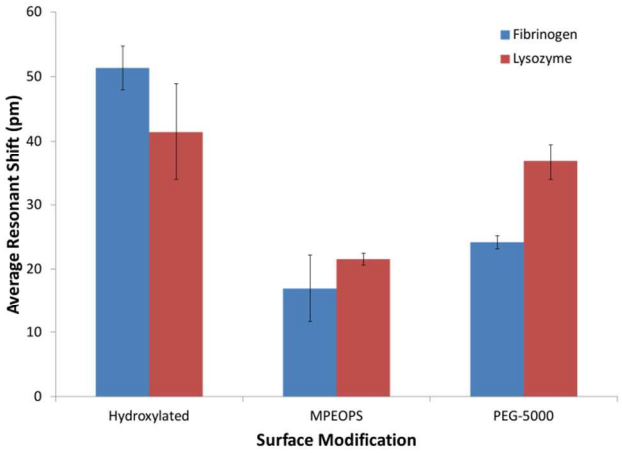

Figure 7. Mean resonant wavelength shift (± standard deviation) during injection of 500 μg/mL lysozyme solution and 10 μg/mL fibrinogen solution (n=3) shows that, in comparison to the control surfaces, MPEOPS and PEG-5000 reduce non-specific adsorption.

As previously mentioned, while the theoretical explanation for the non-fouling characteristics of PEG coatings remains under investigation, it is agreed upon that the non-fouling character is a result of the formation of a strong hydration layer and the steric stabilization effect. Moreover, as a result of the highly dynamic and mobile nature of the PEG layer, it is entropically unfavorable for protein molecules to collect on the PEG surface, as this would reduce chain movement and thus lower the free energy of the system.[46-48] Previous research has confirmed experimentally that long chain polymer coatings are more effective at reducing non-specific protein adsorption than short chain coatings, but that high surface density is more significant than long chain length.[5, 48-49] The impact of chain length and surface density of the grafted polymer molecules has also been examined in relation to the non-fouling nature of different polymer layers.[49-51] Prior examination of the protein repellant properties of PEG suggests that a short chain PEG coating is also an effective method for creation of a non-fouling surface, provided the surface density of the grafted polymer is sufficiently high.[5, 49-50] We hypothesize that our results are due in part to unequal surface densities of short and long chain PEG molecules (MPEOPS and PEG-5000, respectively) resulting from specific factors present in our experiment. First, we believe that the coating

of MPEOPS is significantly denser than the coating of PEG-5000 on the microsphere surface, leading to more PEG functional groups being present. It is more likely that the smaller sized molecules will pack more closely than the larger PEG molecules, especially given the irreversible nature of the attachment strategy and the ability of trialkoxy silanes to oligomerize. This interpretation is supported by the flat surface PEG thickness measurements which showed that the smaller MPEOPS molecules led to a three-fold thicker coating, indicating that the polymers are more fully extended.[35] This type of size dependent packing density and its impact on nonfouling properties has been previously examined theoretically and demonstrated for physically adsorbed polymer coatings.[49, 52] Second, many protocols for long chain silane-PEG attachment onto a hydroxylated surface that show more successful minimization of non-specific binding by fibrinogen suggest that higher temperatures should be used to tether the PEG-5000 to the surface of the biosensor.[35] Higher temperatures will increase the mobility of the polymer chains, allowing better transport to the surface and improvements in the packing density. However due to the delicate nature of the microsphere we were unable to utilize such protocols, as they would cause device damage or sensitivity reduction.[53] Therefore, the gentle PEG-5000 attachment protocols used contributed to the comparative success of the short chain, low molecular weight (MPEOPS) PEG coating to create a superior non-fouling surface as compared to the long chain, high molecular weight (PEG-5000), which is more typical in literature reports. These results indicate that tailoring both the deposition techniques and chain length of the deposition material, to the biosensor platform can dramatically impact the properties of the resulting non-fouling surface.

Conclusions

In this work, we demonstrated that PEG coatings are well-adapted to modify the surface of highly sensitive WGM microcavities, such as the silica microsphere, to create a non-fouling surface that can minimize non-specific adsorption without negatively impacting the overall optical performance of the platform. Experimental results confirmed not only that PEG-functionalization reduced non-specific protein adsorption to the surface of the sensor by as much as a factor of four compared to an initialized

control surface, but also that PEG chain length significantly impacted the nonfouling character of the microcavity surface. Surprisingly, it is the short chain PEG surfaces that experience the best improvement in specificity, unlike many other systems where longer PEG chains are preferred. This result indicates that both the PEG surface deposition technique and chain length need to be tailored to the specific signal transducer if it is to demonstrate high overall performance. Deposition technique plays an especially important role in this system, and had to be tailored to our signal transducers in order to minimize sensitivity losses. The combination of WGM microcavities with PEG coatings tuned specifically to the device will significantly improve the overall performance of these types of label-free optical biosensor platforms, and enable their wider application in complex, real-world monitoring scenarios.

Acknowledgement

We thank Matthew Reddick at the University of Southern California for his creation and support of the LabVIEW programs used in this study. Additionally, we thank Dr. Patrick Pinhero in the Department of Chemical Engineering at the University of Missouri for use of his AFM. Lastly, research was carried out in part at the Center for Micro/Nano Systems and Nanotechnology at the University of Missouri.

Supporting Information Available

Supplemental Information contains the experimental details for functionalizing the device surfaces. This information is available free of charge via the Internet at http://pubs.acs.org/.

References

1. Zalipsky, S.; Harris, J. M., Introduction to Chemistry and Biological Applications of Poly(ethylene glycol). In 1997; Vol. 680, pp 1-13.
2. Zhang, M.; Desai, T.; Ferrari, M., Proteins and cells on PEG immobilized silicon surfaces. *Biomaterials* **1998,** 19, (10), 953-960.
3. Chapman, R. G.; Ostuni, E.; Takayama, S.; Holmlin, R. E.; Yan, L.; Whitesides, G. M., Surveying for surfaces that resist the adsorption of proteins [3]. *Journal of the American Chemical Society* **2000,** 122, (34), 8303-8304.

4. Ostuni, E.; Chapman, R. G.; Holmlin, R. E.; Takayama, S.; Whitesides, G. M., A survey of structure-property relationships of surfaces that resist the adsorption of protein. *Langmuir* **2001,** 17, (18), 5605-5620.
5. Prime, K. L.; Whitesides, G. M., Adsorption of proteins onto surfaces containing end-attached oligo(ethylene oxide): A model system using self-assembled monolayers. *Journal of the American Chemical Society* **1993,** 115, (23), 10714-10721.
6. Wisniewski, N.; Reichert, M., Methods for reducing biosensor membrane biofouling. *Colloids and Surfaces B: Biointerfaces* **2000,** 18, (3-4), 197-219.
7. Thierry, B.; Zimmer, L.; McNiven, S.; Finnie, K.; Barbé, C.; Griesser, H. J., Electrostatic self-assembly of PEG copolymers onto porous silica nanoparticles. *Langmuir* **2008,** 24, (15), 8143-8150.
8. Li, L.; Chen, S.; Jiang, S., Protein interactions with oligo(ethylene glycol) (OEG) self-assembled monolayers: OEG stability, surface packing density and protein adsorption. *Journal of Biomaterials Science, Polymer Edition* **2007,** 18, (11), 1415-1427.
9. Green, R. J.; Davies, J.; Davies, M. C.; Roberts, C. J.; Tendler, S. J. B., Surface plasmon resonance for real time in situ analysis of protein adsorption to polymer surfaces. *Biomaterials* **1997,** 18, (5), 405-413.
10. Bagwe, R. P.; Hilliard, L. R.; Tan, W., Surface modification of silica nanoparticles to reduce aggregation and nonspecific binding. *Langmuir* **2006,** 22, (9), 4357-4362.
11. Green, R. J.; Frazier, R. A.; Shakesheff, K. M.; Davies, M. C.; Roberts, C. J.; Tendler, S. J. B., Surface plasmon resonance analysis of dynamic biological interactions with biomaterials. *Biomaterials* **2000,** 21, (18), 1823-1835.
12. De Vos, K.; Girones, J.; Popelka, S.; Schacht, E.; Baets, R.; Bienstman, P., SOI optical microring resonator with poly(ethylene glycol) polymer brush for label-free biosensor applications. *Biosensors and Bioelectronics* **2009,** 24, (8), 2528-2533.
13. Bernards, M. T.; Cheng, G.; Zhang, Z.; Chen, S.; Jiang, S., Nonfouling polymer brushes via surface-initiated, two-component atom transfer radical polymerization. *Macromolecules* **2008,** 41, (12), 4216-4219.
14. Ladd, J.; Zhang, Z.; Chen, S.; Hower, J. C.; Jiang, S., Zwitterionic polymers exhibiting high resistance to nonspecific protein adsorption from human serum and plasma. *Biomacromolecules* **2008,** 9, (5), 1357-1361.
15. Fan, X. D.; White, I. M.; Shopoua, S. I.; Zhu, H. Y.; Suter, J. D.; Sun, Y. Z., Sensitive optical biosensors for unlabeled targets: A review. *Analytica Chimica Acta* **2008,** 620, (1-2), 8-26.
16. Senaratne, W.; Andruzzi, L.; Ober, C. K., Self-assembled monolayers and polymer brushes in biotechnology: Current applications and future perspectives. *Biomacromolecules* **2005,** 6, (5), 2427-2448.
17. Vaisocherová, H.; Yang, W.; Zhang, Z.; Cao, Z.; Cheng, G.; Piliarik, M.; Homola, J.; Jiang, S., Ultralow fouling and functionalizable surface chemistry based on a zwitterionic polymer enabling sensitive and specific protein detection in undiluted blood plasma. *Analytical Chemistry* **2008,** 80, (20), 7894-7901.
18. Gobi, K. V.; Iwasaka, H.; Miura, N., Self-assembled PEG monolayer based SPR immunosensor for label-free detection of insulin. *Biosensors & Bioelectronics* **2007,** 22, (7), 1382-1389.
19. Hunt, H. K.; Armani, A. M., Label-free biological and chemical sensors. *Nanoscale* **2010,** 2, 1544-1559.
20. Hanumegowda, N. M.; White, I. M.; Oveys, H.; Fan, X. D., Label-free protease sensors based on optical microsphere resonators. *Sensor Letters* **2005,** 3, (4), 315-319.
21. Soria, S.; Berneschi, S.; Brenci, M.; Cosi, F.; Nunzi Conti, G.; Pelli, S.; Righini, G. C., Optical Microspherical Resonators for Biomedical Sensing. *Sensors* **2011,** 11, (1), 785-805.
22. Zhu, H.; White, I. M.; Suter, J. D.; Zourob, M.; Fan, X., Opto-fluidic micro-ring resonator for sensitive label-free viral detection. *The Analyst* **2008,** 133, 356-360.

23. Washburn, A. L.; Luchansky, M. S.; Bowman, A. L.; Bailey, R. C., Quantitative, Label-Free Detection of Five Protein Biomarkers Using Multiplexed Arrays of Silicon Photonic Microring Resonators. *Analytical Chemistry* **2010,** 82, (1), 69-72.
24. Shi, C.; Mehrabani, S.; Armani, A. M., Leveraging Bimodal Kinetics to Improve Detection Specificity. *Optics Letters* **2012,** 37, (10).
25. Matsko, A. B.; Ilchenko, V. S., Optical resonators with whispering-gallery modes-part I: basics. *Selected Topics in Quantum Electronics, IEEE Journal of* **2006,** 12, (1), 3-14.
26. Hu, J.; Sun, X.; Agarwal, A.; Kimerling, L. C., Design guidelines for optical resonator biochemical sensors. *J. Opt. Soc. Am. B* **2009,** 26, (5), 1032-1041.
27. Ilchenko, V. S.; Maleki, L., Novel whispering-gallery resonators for lasers, modulators, and sensors. *Proceedings of SPIE: Laser Resonators IV* **2001,** 4270, 120-130.
28. Ilchenko, V. S.; Matsko, A. B., Optical resonators with whispering-gallery modes-part II: applications. *Selected Topics in Quantum Electronics, IEEE Journal of* **2006,** 12, (1), 15-32.
29. Cheema, M. I.; Mehrabani, S.; Hayat, A. A.; Peter, Y.-A.; Armani, A. M.; Kirk, A. G., Simulataneous Measurement of Quality Factor and Wavelength Shift by Phase Shift Microcavity Ring Down Spectroscopy. *Optics Express* **2012,** 20, (8), 9090-9098.
30. Gorodetsky, M. L.; Savchenkov, A. A.; Ilchenko, V. S., Ultimate Q of optical microsphere resonators. *Optics Letters* **1996,** 21, (7), 453-455.
31. Vollmer, F.; Arnold, S.; Keng, D., Single virus detection from the reactive shift of a whispering gallery mode. *Proceedings of the National Academy of Sciences of the United States of America* **2008,** 105, (52), 20701-20704.
32. Wilson, K. A.; Finch, C. A.; Anderson, P.; Vollmer, F.; Hickman, J. J., Whispering gallery mode biosensor quantification of fibronectin adsorption kinetics onto alkylsilane monolayers and interpretation of resultant cellular response. *Biomaterials* **2012,** 33, (1), 225-236.
33. Soteropulos, C. E., Hunt, H. K., Attaching Biological Probes to Silica Optical Biosensors Using Silane Coupling Agents. *Journal of Visualized Experiments* **2012**.
34. Papra, A.; Gadegaard, N.; Larsen, N. B., Characterization of ultrathin poly(ethylene glycol) monolayers on silicon substrates. *Langmuir* **2001,** 17, (5), 1457-1460.
35. Yang, Z., Galloway, Jeffrey A., Yu, Hyuk, Protein Interactions with Poly(ethylene glycol) Self-Assembled Monolayers on Glass Substrates: Diffusion and Adsorption. *Langmuir* **1999,** 15, 8405-8411.
36. Knight, J. C.; Cheung, G.; Jacques, F.; Birks, T. A., Phase-matched excitation of whispering-gallery-mode resonances by a fiber taper. *Optics Letters* **1997,** 22, (15), 1129-1131.
37. Yariv, A., Universal relations for coupling of optical power between microresonators and dielectric waveguides (vol 36, pg 321, 2000). *Electronics Letters* **2000,** 36, (11), 999-999.
38. Little, B. E.; Laine, J. P.; Haus, H. A., Analytic theory of coupling from tapered fibers and half-blocks into microsphere resonators. *Journal of Lightwave Technology* **1999,** 17, (4), 704-715.
39. Armani, D. K.; Kippenberg, T. J.; Spillane, S. M.; Vahala, K. J., Ultra-high-Q toroid microcavity on a chip. *Nature* **2003,** 421, (6926), 925-928.
40. Armani, A. M.; Armani, D. K.; Min, B.; Vahala, K. J.; Spillane, S. M., Ultra-high-Q microcavity operation in H_2O and D_2O. *Applied Physics Letters* **2005,** 87, (15).
41. Soteropulos, C. E.; Hunt, H. K.; Armani, A. M., Determination of binding kinetics using whispering gallery mode microcavities. *Applied Physics Letters* **2011,** 99, (10).
42. Washburn, A. L.; Bailey, R. C., Photonics-on-a-chip: Recent advances in integrated waveguides as enabling detection elements for real-world, lab-on-a-chip biosensing applications. *Analyst* **2011,** 136, (2), 227-236.
43. Sun, Y.; Fan, X., Optical ring resonators for biochemical and chemical sensing. *Analytical and Bioanalytical Chemistry* **2011,** 399, (1), 205-211.
44. Sota, H.; Hasegawa, Y.; Iwakura, M., Detection of Conformational Changes in an Immobilized Protein Using Surface Plasmon Resonance. *Analytical Chemistry* **1998,** 70, (10), 2019-2024.

45. Li, L.; Chen, S.; Zheng, J.; Ratner, B. D.; Jiang, S., Protein adsorption on oligo(ethylene glycol)-terminated alkanethiolate self-assembled monolayers: The molecular basis for nonfouling behavior. *Journal of Physical Chemistry B* **2005,** 109, (7), 2934-2941.
46. De Gennes, P. G., Polymers at an interface. 2. Interaction between two plates carrying adsorbed polymer layers. *Macromolecules* **1982,** 15, (2), 492-500.
47. De Gennes, P. G., Polymer solutions near an interface. 1. Adsorption and depletion layers. *Macromolecules* **1981,** 14, (6), 1637-1644.
48. Andrade, J. D.; Hlady, V.; Jeon, S. I., Poly(ethylene oxide) and protein resistance principles, problems, and possibilities. *Advances in Chemistry Series* **1996,** 248, 57-59.
49. Jeon, S. I.; Lee, J. H.; Andrade, J. D.; De Gennes, P. G., Protein-surface interactions in the presence of polyethylene oxide. I. Simplified theory. *Journal of Colloid and Interface Science* **1991,** 142, (1), 149-158.
50. Malmsten, M.; Emoto, K.; Van Alstine, J. M., Effect of chain density on inhibition of protein adsorption by poly(ethylene glycol) based coatings. *Journal of Colloid and Interface Science* **1998,** 202, (2), 507-517.
51. Jeon, S. I.; Andrade, J. D., Protein-surface interactions in the presence of polyethylene oxide. II. Effect of protein size. *Journal of Colloid and Interface Science* **1991,** 142, (1), 159-166.
52. Chang, Y.; Chen, S.; Zhang, Z.; Jiang, S., Highly protein-resistant coatings from well-defined diblock copolymers containing sulfobetaines. *Langmuir* **2006,** 22, (5), 2222-2226.
53. Hunt, H. K.; Soteropulos, C.; Armani, A. M., Bioconjugation Strategies for Microtoroidal Optical Resonators. *Sensors.* **2010,** 10, 9317-9336.

TOC Graphic

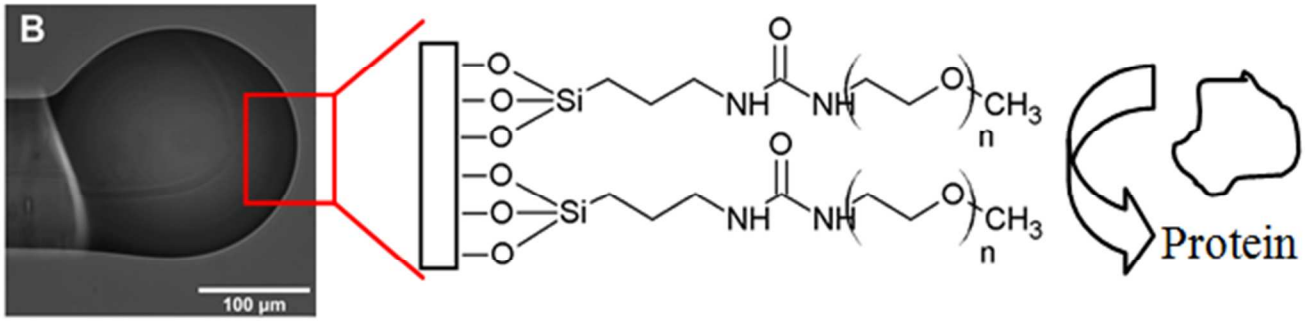

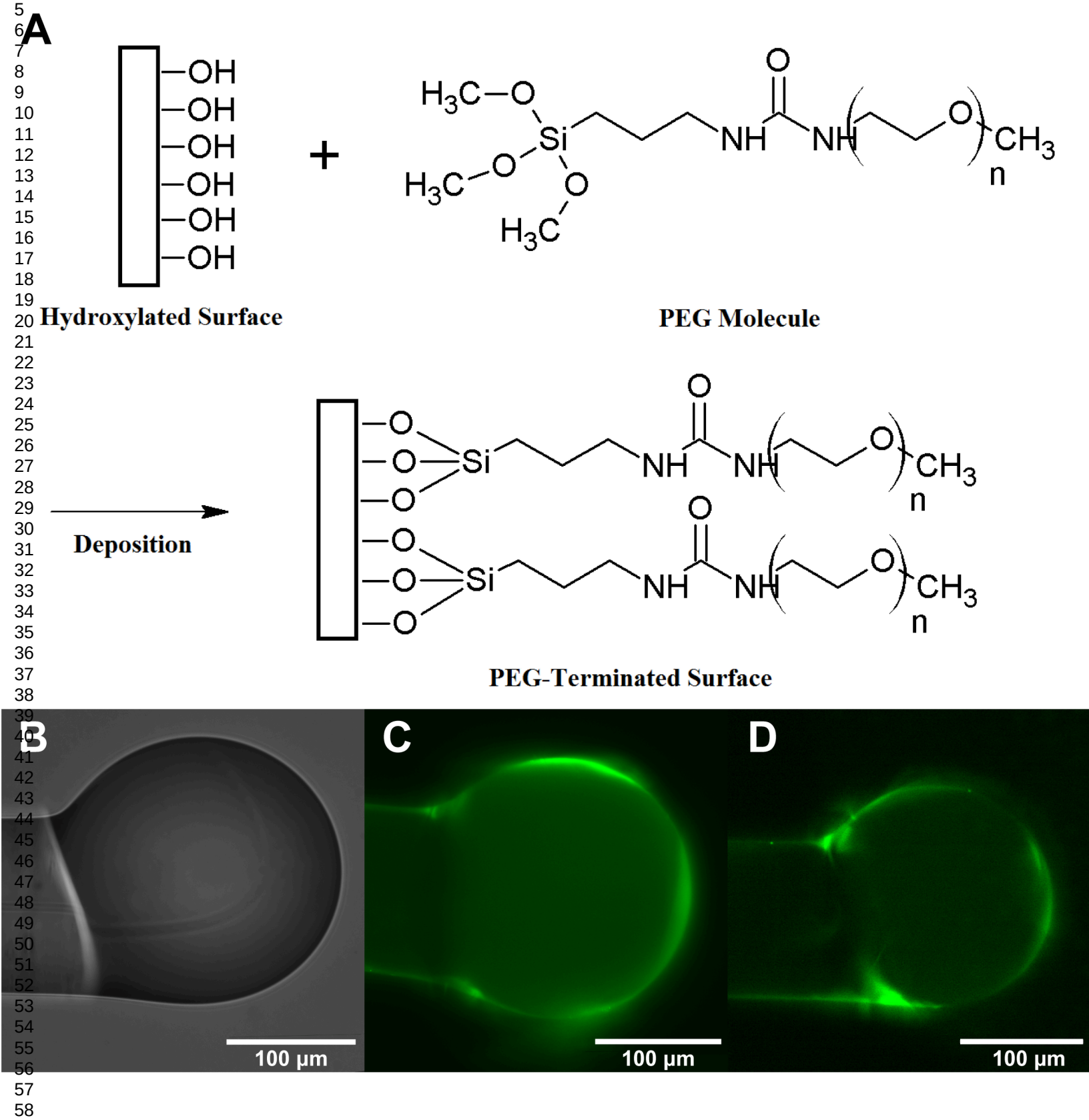
A
OH
OH
OH
OH
OH
OH
+
H_3C-O
Si
H_3C-O
O
H_3C
O
NH
NH
O
CH_3
n
Hydroxylated Surface
PEG Molecule
Deposition
O
O
O
Si
O
O
O
Si
NH
NH
O
CH_3
n
PEG-Terminated Surface
B
100 µm
C
100 µm
D
100 µm

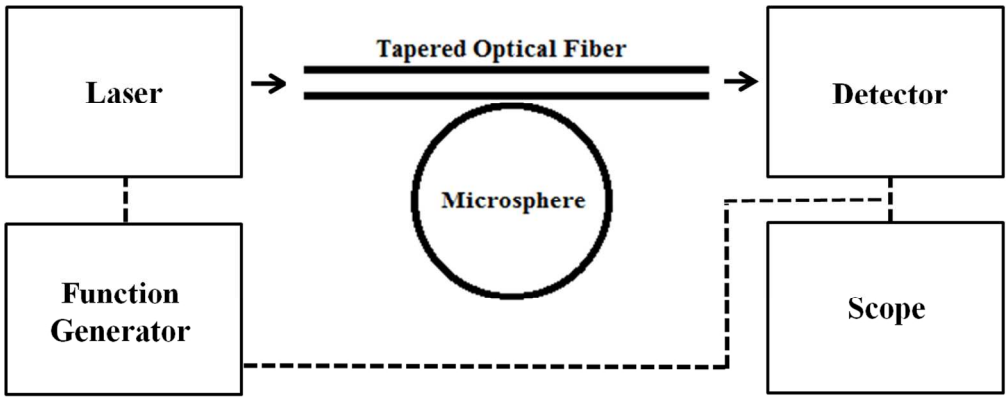

281x110mm (120 x 120 DPI)

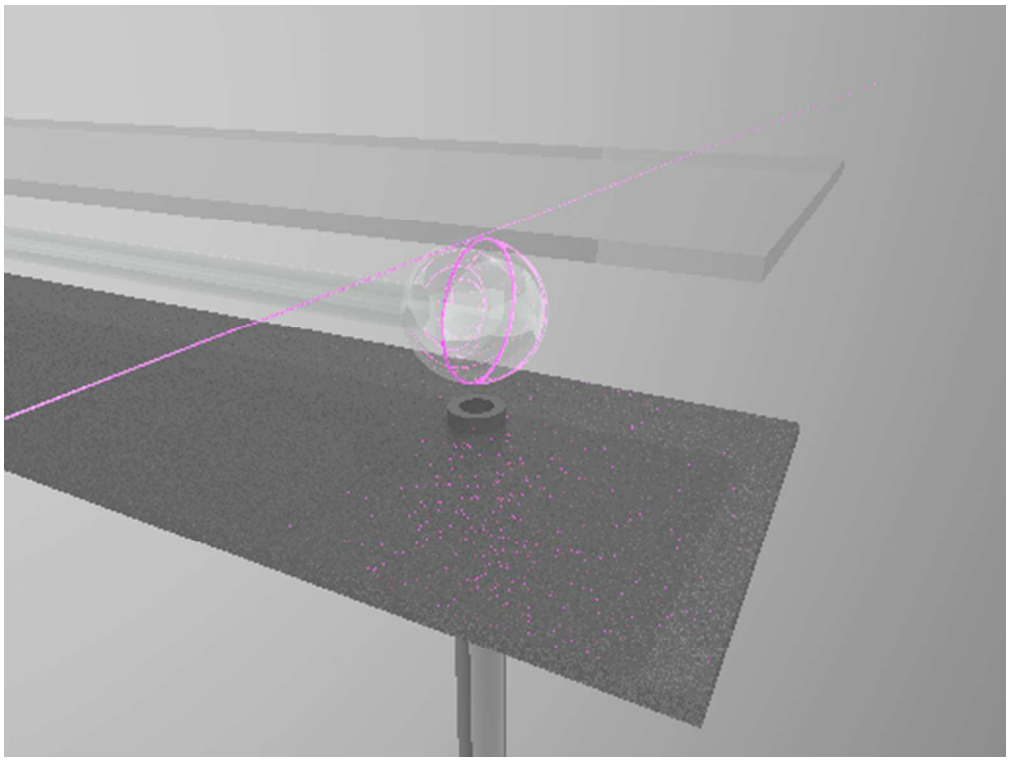

180x135mm (72 x 72 DPI)

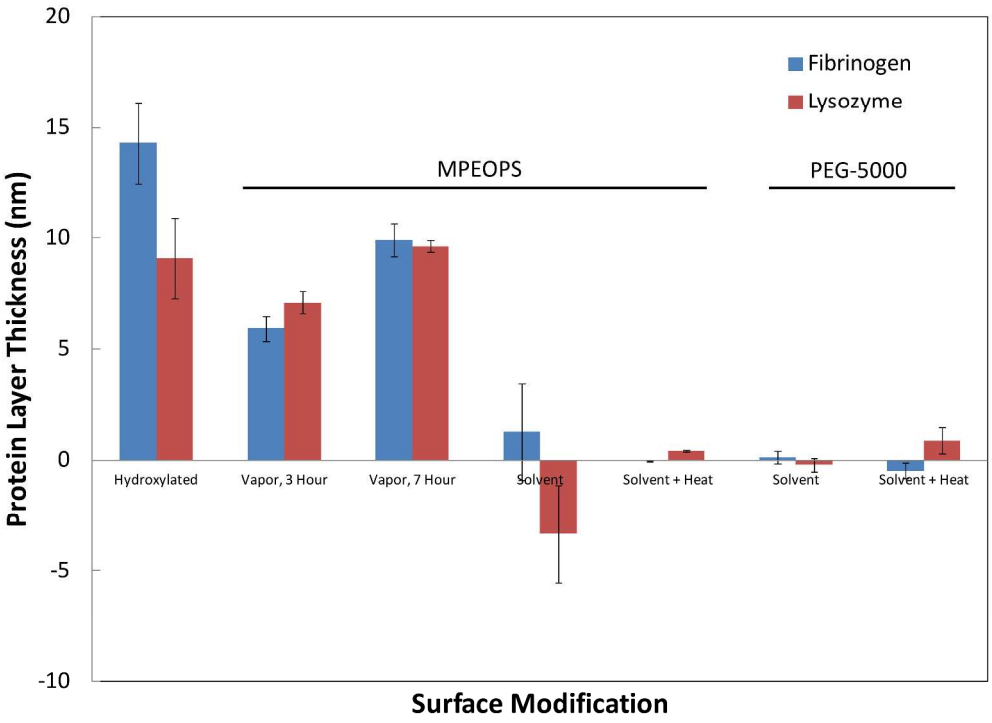

623x444mm (300 x 300 DPI)

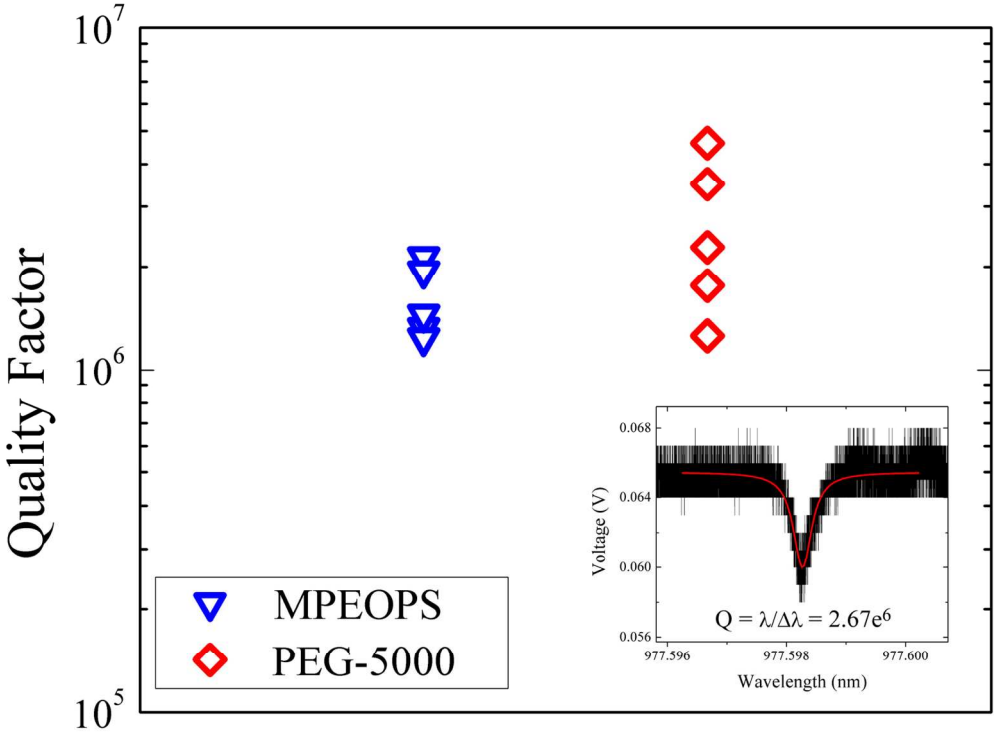

71x54mm (600 x 600 DPI)

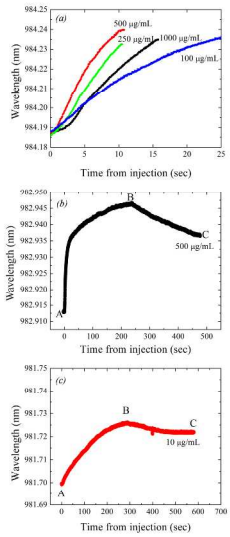

304x304mm (300 x 300 DPI)

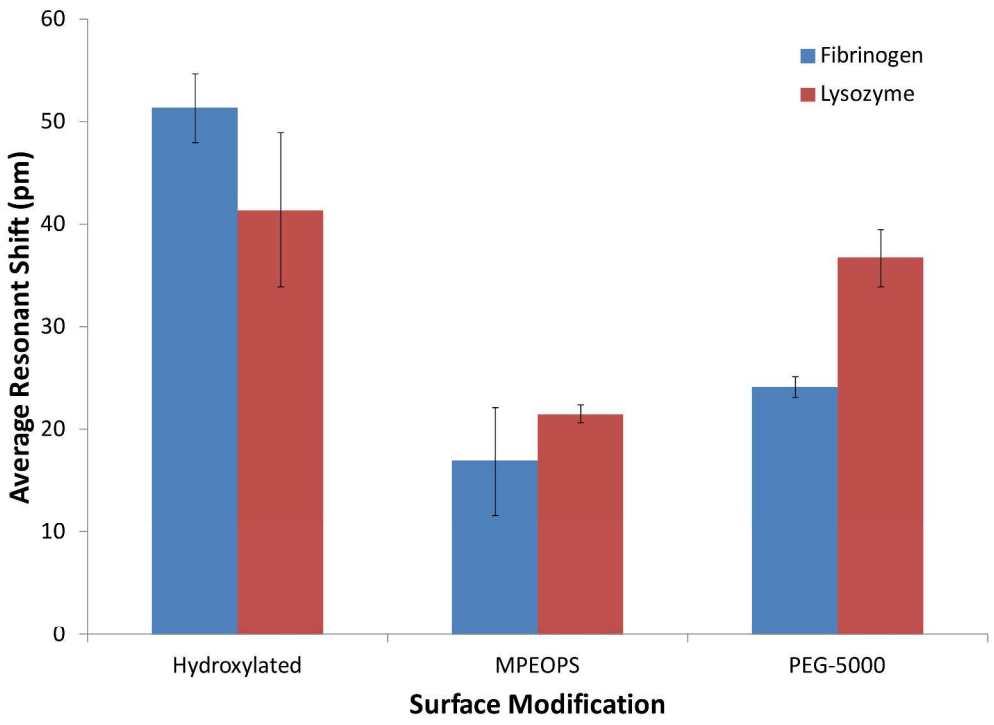

626x455mm (300 x 300 DPI)

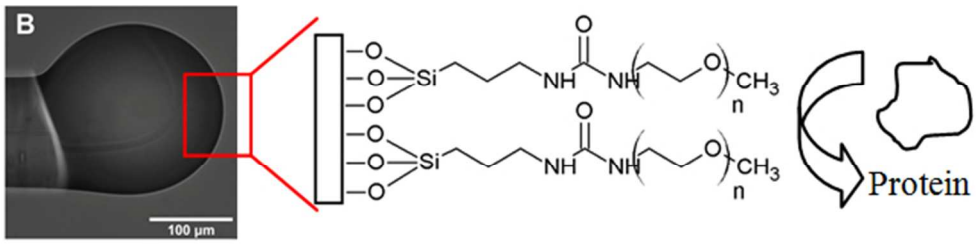

231x55mm (72 x 72 DPI)